THE JOURNAL OF BIOLOGICAL CHEMISTRY VOL. 283, NO. 14, pp. 9289–9299, April 4, 2008

Glutamate Uptake and Release by Astrocytes Are Enhanced by *Clostridium botulinum* C3 Protein*

Received for publication, August 6, 2007, and in revised form, January 15, 2008 Published, JBC Papers in Press, January 30, 2008, DOI 10.1074/jbc.M706499200

Markus Höltje[‡1], **Fred Hofmann**[§], **Romy Lux**[‡], **Rüdiger W. Veh**[‡], **Ingo Just**[§], **and Gudrun Ahnert-Hilger**[‡]

From the [‡]*Centrum für Anatomie, Institut für Integrative Neuroanatomie, Charité-Universitätsmedizin Berlin, Philippstrasse 12, 10115 Berlin, Germany and the* [§]*Institut für Toxikologie der Medizinischen Hochschule Hannover, Carl-Neuberg-Strasse 1, 30625 Hannover, Germany*

Inhibition of Rho activity by *Clostridium botulinum* C3 transferase (C3bot) versatily changes functional properties of neural cells. Using cultivated mouse astrocytes, we show here that C3bot increases both uptake and secretion of glutamate. The enhanced glutamate uptake is initiated by an NFκB-dependent up-regulation of the glial glutamate transporter 1 that is efficaciously sorted to the plasma membrane. The increase in cytosolic glutamate concentration promotes vesicular glutamate storage in astrocytes treated with C3bot. Parallel to the increased storage, C3-induced impairment of Rho-dependent pathways strongly enhances Ca^{2+}-dependent secretion of glutamate. This is accompanied by higher levels of the SNARE protein synaptobrevin. Synaptobrevin inactivation by botulinum neurotoxin D almost completely inhibits Ca^{2+}-dependent glutamate secretion triggered by C3bot, indicating that the enhanced release of glutamate mainly originates from exocytosis. In addition, C3bot increases the exocytosis/endocytosis turnover, as analyzed by the stimulated accumulation of the fluorescent dye AM1-43. The release of glutamine, the main metabolite of glutamate, is only moderately affected by C3bot. In conclusion, inhibition of Rho-dependent pathways shifts astrocytes to a secretory active stage in which they may modulate neuronal excitability.

Brain function is based on communication between neurons as well as on the interaction of neurons and their collaborating glial cells. Glutamatergic synapses, for example, are ensheathed by glial processes isolating individual synapses from one another (1, 2). The use of the ubiquitous amino acid glutamate both as a metabolite and, even more importantly, as the principal excitatory transmitter of the central nervous system requires efficient mechanisms to maintain a high signal-to-noise ratio and to prevent neuronal damage caused by high excitotoxic extracellular glutamate concentrations (3). Crucial elements for limiting the action of glutamate as a neurotransmitter and to maintain low concentrations in the extracellular space of the brain are the high affinity glutamate transporters GLAST and GLT-1 expressed at the plasma membrane of astrocytes and Bergmann glia cells (4, 5). In recent years evidence has accumulated that astrocytes, besides their capacity to take up glutamate at the plasma membrane, also contain a vesicular compartment equipped with glutamate transporter subtypes for vesicular storage (VGLUTs)[2] (6). Since then, many groups have shown that glutamate can be transported into and released from these vesicles by Ca^{2+}-dependent exocytosis (7–9). Other, nonvesicular mechanisms of glutamate release from astrocytes like efflux through volume-sensitive channels have also been described (10). Besides their role in responding to and modulating synaptic transmission by glutamate uptake and release (11, 12) glial cells like astrocytes may also become involved in the formation and maintenance of synapses (13, 14). Uptake of glutamate is linked to conversion into glutamine by astroglial glutamine synthetase, followed by the efflux into the extracellular space. Glutamine can be then taken up by neurons and can be reconverted into glutamate to replenish neuronal glutamate and GABA pools (15).

Expression and function of high affinity glutamate transporters have been reported to be highly variable. Various substances and conditions result in altered gene expression, protein levels, and activity of GLAST and GLT-1 (for a review, see Refs. 16 and 17). Largely unexplored, however, is the regulation of glutamate transport and subsequent release by small GTPases, such as the Rho family proteins. Well established, on the other hand, is the important role of Rho proteins during fundamental morphological changes astrocytes can undergo. After inhibition of Rho-dependent pathways, cultivated astrocytes acquire a stellate morphology (18–20). It was tempting to investigate whether these distinct morphological changes are accompanied by alterations of major astrocytic functional tasks, such as glutamate storage and glutamate/glutamine release. In order to gain insights into the impact of Rho signaling on glutamate transporter regulation, we used *Clostridium botulinum* C3 transferase (C3bot), which specifically ADP-ribosylates and thereby inactivates small GTPases of the Rho subfamily (RhoA, -B, and -C; see Refs. 21–23). Since inhibition of RhoA by C3 proteins has proven to be beneficial for axon outgrowth during development or regeneration (24, 25) we were particularly interested to investigate possible effects of C3bot on astrocyte functions that are known to be associated with neurodegenerating diseases when malfunctioning. This is in fact the case for astrocytic glu-

* This work was supported by Deutsche Forschungsgemeinschaft Grants AH67/4 and JU231/4. The costs of publication of this article were defrayed in part by the payment of page charges. This article must therefore be hereby marked "*advertisement*" in accordance with 18 U.S.C. Section 1734 solely to indicate this fact.

[1] To whom correspondence should be addressed. Tel.: 49-30-450528356; Fax: 49-30-450528912; E-mail: markus.hoeltje@charite.de.

[2] The abbreviations used are: VGLUT, glutamate transporter subtype for vesicular storage; C3bot, *C. botulinum* C3 transferase; PDC, L-*trans*-pyrrolidine-2,4-dicarboxylic acid; DHK, dihydrokainic acid; PDTC, ammonium pyrrolidine dithiocarbamate; BoNt/D, botulinum neurotoxin D; GFAP, glial fibrillary acidic protein.

tamate transport systems in, for example, Alzheimer disease or amyotrophic lateral sclerosis (5).

EXPERIMENTAL PROCEDURES

Astrocyte Cultures

Primary astrocyte cultures were prepared from NMRI mice brains between postnatal days 2 and 3. After removal of meninges, brains were mechanically dissociated in Hanks' buffered salt solution by fire-polished Pasteur pipettes and centrifuged at 300 × *g* for 3 min. Cells were redissociated in Hanks' buffered salt solution, and the procedure was repeated two times using smaller pipette tip diameters. Cells were first seeded onto 6-well plates (3.5-cm diameter/well) pretreated with poly-L-lysine (100 μg/ml in phosphate-buffered saline). Astrocytes were incubated at 5% CO_2 in Dulbecco's modified Eagle's medium, supplemented with 10% fetal calf serum, 100 units/ml penicillin/streptomycin, and 2 mM L-glutamine. Microglial cells were repeatedly detached from the astrocyte monolayer by shaking off. After 5 days in culture with a change of medium two times, cells were harvested and recultured in 24-well plates at a density of 4×10^4 cells/well with or without glass coverslips pretreated with poly-L-lysine. Cultures treated either with or without *C. botulinum* C3 protein (80 nM final concentration) were kept under serum-free conditions for the indicated time periods.

Expression of Recombinant C3bot Protein

C3bot was expressed as recombinant glutathione *S*-transferase fusion proteins in *Escherichia coli* TG1 harboring the respective DNA fragment in the plasmid pGEX-2T (see Ref. 20). Glutathione *S*-transferase was removed by thrombin cleavage.

Chemicals and Antibodies

L-*trans*-Pyrrolidine-2,4-dicarboxylic acid (PDC), dihydrokainic acid (DHK), DL-threo-β-benzyloxyaspartic acid, and ammonium pyrrolidine dithiocarbamate (PDTC) were purchased from Tocris. Ionomycin and bafilomycin A1 were obtained from Sigma. Tritiated [3,4-^{3}H]L-glutamic acid (40 Ci/mmol) was obtained from Moravek Biochemicals. Botulinum neurotoxin D (BoNt/D) was a gift from H. Bigalke (Institute for Toxicology, Medizinische Hochschule Hannover). AM1-43 was from Biotium.

Both monoclonal and polyclonal antibodies directed against glial fibrillary acidic protein (GFAP) used to label astrocytes as well as a polyclonal antibody against actin were purchased from Sigma. Polyclonal antisera obtained from Chemicon (Temecula) were used for detection of glutamate-aspartate transporter GLAST and glial glutamate transporter GLT-1. A monoclonal antibody against RhoA was purchased from Santa Cruz Biotechnology, Inc. (Santa Cruz, CA). α-Tubulin was detected using a monoclonal antibody obtained from Sigma. Monoclonal antibodies against the vesicular glutamate transporters VGLUT1 and VGLUT2 as well as a polyclonal antiserum against VGLUT3 were obtained from Synaptic Systems (Göttingen, Germany). Detection of NFκB was performed using a mouse monoclonal antibody against the p65 subunit available from Santa Cruz Biotechnology. A polyclonal antiserum against Synaptobrevin II (106.5) was a gift from R. Jahn (Göttingen, Germany). Monoclonal antibodies against syntaxin I as well as a polyclonal anti-SNAP23 antiserum were from Synaptic Systems.

Immunocytochemistry

Cells were fixed with 4% formaline for 15 min and subsequently permeabilized for 30 min at room temperature using 0.3% Triton X-100 dissolved in phosphate-buffered saline. Astrocytes were stained with primary antibodies overnight at 4 °C. After washing in phosphate-buffered saline, secondary antibodies were applied for 1 h at room temperature. Immunoreactivity was visualized using goat anti-mouse, goat anti-rabbit, or goat anti-guinea pig Alexa Fluor 488 IgG for green fluorescence. Goat anti-mouse or goat anti-rabbit Alexa Fluor 594 (Molecular Probes, Inc., Eugene, OR) was applied for red fluorescence. Fluorescence was visualized either by using an upright Leica DMLB epifluorescence equipment or by using confocal laser-scanning microscopy (see below).

Confocal Laser-scanning Microscopy

For acquisition of images, a Leica TCS SL confocal laser-scanning microscope using a ×40 oil immersion objective was used. Fluorescent dyes were excited at a wavelength of 488 nm (green fluorescence) and 543 nm (red fluorescence), respectively. Fluorescence from green and red channels was collected sequentially using two filters at 498–535 and 587–666 nm, respectively. Images were captured at a resolution of 1024 × 1024 pixels.

Western Blotting

Astrocyte homogenates were loaded onto 10 or 12% gels (40 μg/lane) for SDS-PAGE. Protein was immobilized on nitrocellulose membrane. Membranes were blocked with Tris-buffered saline, including 5% low fat milk and 0.1% Tween 20 for 1 h at room temperature. Incubation with the primary antibodies was performed overnight at 4 °C. After washing with blocking solution, membranes were incubated with secondary antibodies for 1 h at room temperature (horseradish peroxidase-labeled anti-rabbit, anti-guinea pig, or anti-mouse IgG; Vector Laboratories, Burlingame, CA). Visualization was performed using the ECL detection system (Amersham Biosciences).

Transfections

After 10 days in culture, astrocytes grown on coverslips were transfected with RhoA wild type, RhoA V14, RhoA N19, Rac1 wild type, Rac1 V12, or Rac1 N17 DNA cloned into pEGFP-C1 expression vector using the Effectene transfection reagent (Qiagen, Hilden, Germany) according to the manufacturer's instructions. Expression time was kept at 24 h. Cells were fixed and counterstained for NFκB or GLT-1 expression. Transfection efficiency was between 10 and 15%. Effects on NFκB translocation as well as GLT-1 expression were quantified by counting transfected cells within individual fields of view using a ×20 objective. Typically, cells from 10 fields of view (representing a total of 80–120 cells) per condition were analyzed for the respective phenotype within single experiments.

[^{3}H]Glutamate Uptake/Secretion Assays

Uptake—Usually, for glutamate uptake, astrocytes grown in 24-well plates were incubated with 50 μM glutamate (applied as

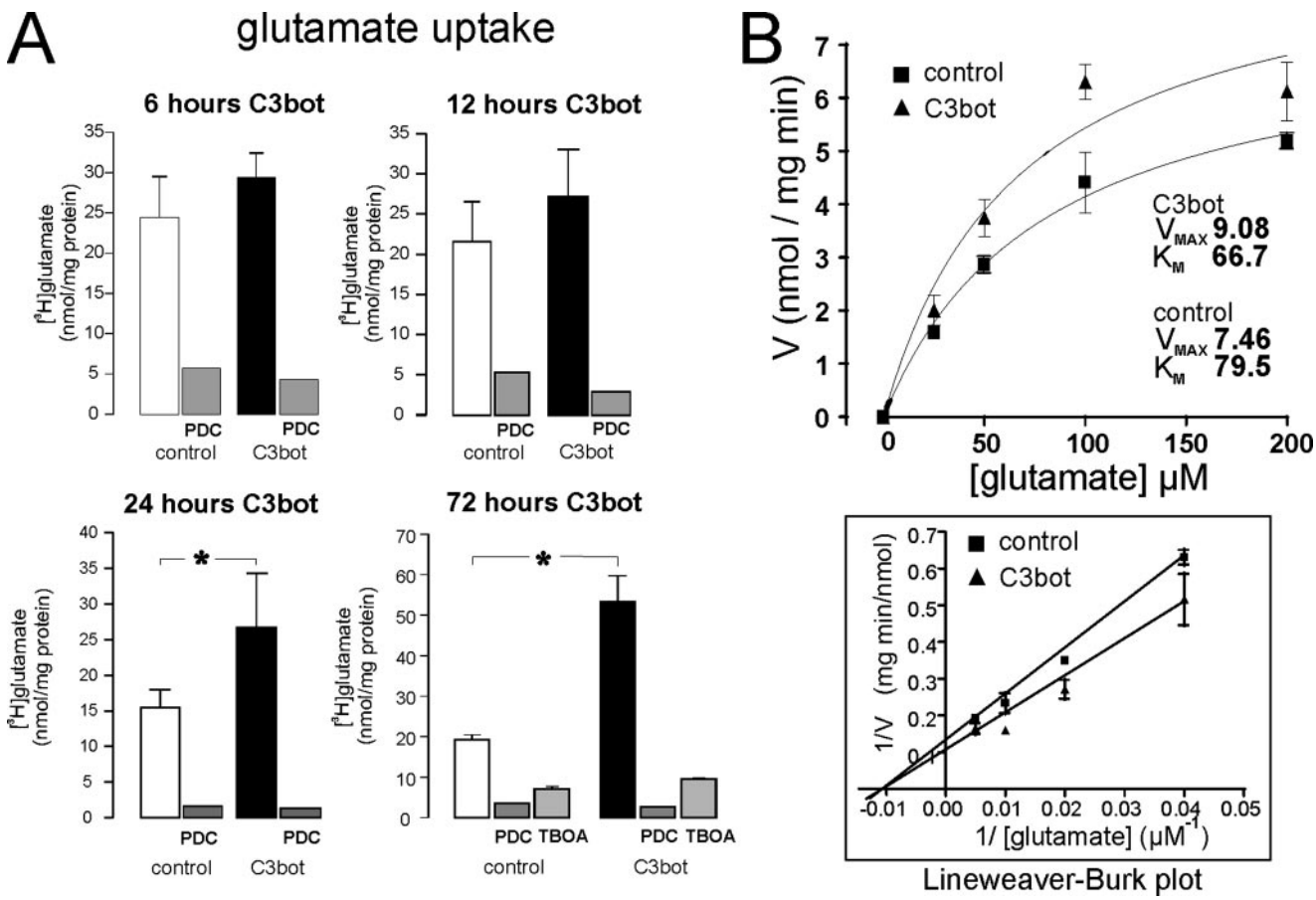

FIGURE 1. **Astrocytes treated with C3bot exhibit an enhanced glutamate uptake activity.** *A*, control astrocyte cultures or cultures treated with 80 nM C3bot for increasing durations were incubated with 50 μM [^{3}H]glutamate for 1 h. The amount of [^{3}H]glutamate taken up by astrocytes was determined from lysed cells. PDC (1 mM) or DL-threo-β-benzyloxyaspartic acid (*TBOA*; 1 mM) was used to inhibit plasma membrane transport activity. Prolonged incubation times with C3bot resulted in an enhanced glutamate uptake. *B*, kinetic analysis by nonlinear regression reveals that the C3bot-mediated increased uptake of [^{3}H]glutamate is based on an increased transport velocity as indicated by a higher V_{max} value as well as a higher substrate affinity indicated by a lower K_m value.

a combination of both tritiated and unlabeled glutamic acid) for 1 h with or without additives, as indicated, at 37 °C in serum-free culture medium. For kinetic analysis of transport activity, the uptake time was shortened to 10 min. Graph Pad Prism software (San Diego, CA) was used for nonlinear regression and transformation of data. After removal of the medium and repeated washing (three times) with ice-cold Krebs-Hepes buffer containing 140 mM NaCl, 4.7 mM KCl, 2.5 mM $CaCl_2$, 15 mM Hepes, and 1.2 mM $MgSO_4$ adjusted to pH 7.4, cells were lysed with 0.4% Triton X-100 for 10 min at 42 °C. Astrocyte lysates were subjected to liquid scintillation counting for determination of radioactivity. Values were adjusted to protein content.

Secretion—Astrocytes were loaded as described for 1 h with 50 μM glutamate. After removal of the medium and repeated washing, cultures were incubated with Krebs-Hepes buffer containing either no additives, the calcium-ionophore ionomycin (1.3 μM), or ATP (2 mM) for 10 min at 37 °C. Supernatants were collected, subjected to liquid scintillation counting, and adjusted to protein content of the lysed cells.

Ion Exchange Chromatography

Radioactive glutamine and glutamate released in culture supernatants were separated by ion exchange chromatography, using small (5 × 50-mm) columns with a strong anion exchanger (Q Sepharose® Fast Flow; Amersham Biosciences), equilibrated with 20 mM acetate buffer, pH 6.0 (sample buffer). Columns were loaded with 500 μl (2 × 250 μl) of culture supernatant samples, diluted in sample buffer containing 10 mM unlabeled glutamine and glutamate as carrier substances. After six washes with sample buffer (500 μl each), the columns were eluted with six 500-μl volumes of 200 mM acetate buffer, pH 3.7 (elution buffer). 500-μl fractions were collected, and radioactivity was determined by liquid scintillation counting. Complete separation of glutamine from glutamate was verified in control experiments, using two columns loaded with either 20 mM glutamine or glutamate, respectively. Fractions were collected, and amine groups were determined photometrically at 420 nm using the TNBS (2,4,6-trinitrobenzenesulfonic acid) method (26).

Vesicular AM1-43 Staining

AM1-43 represents a fixable version of the cationic styryl dye FM1-43 (27). Cultivated astrocytes were loaded for 1 min with 4 μM of AM1-43 dissolved in Krebs-Hepes buffer containing no additives or 1.3 μM ionomycin to stimulate Ca^{2+}-dependent release at room temperature. After a single washing step, astrocytes were incubated for 4 min with a 0.5 μM concentration of

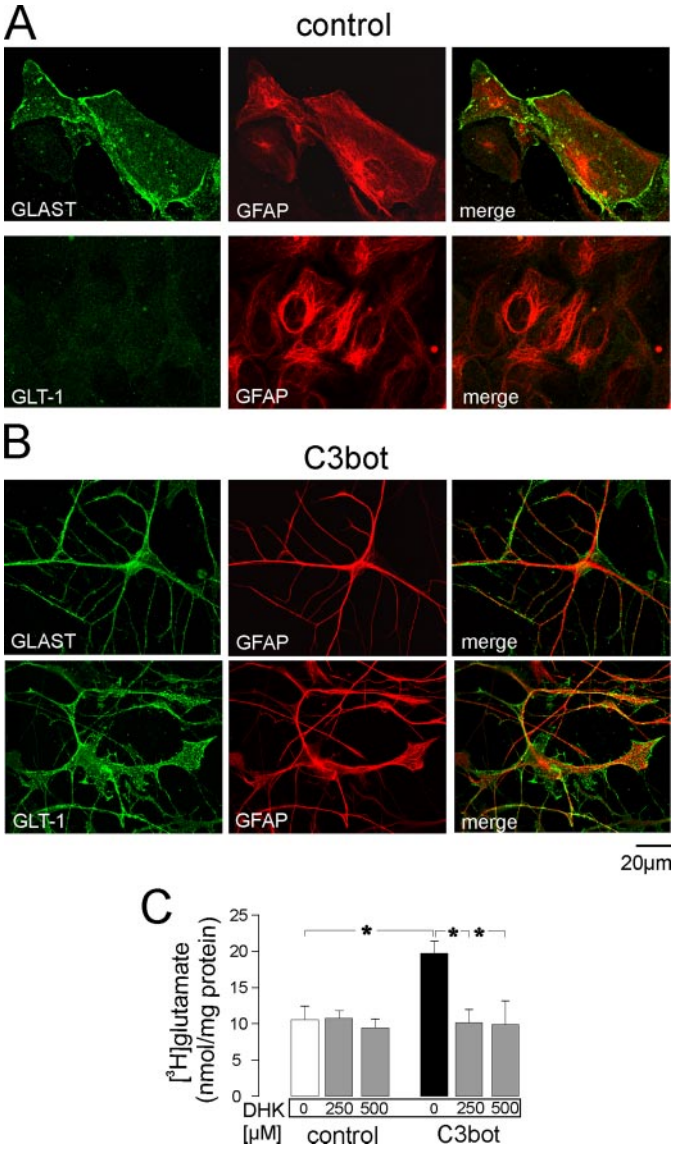

FIGURE 2. **Enhanced C3bot-induced glutamate uptake is mediated by GLT-1.** *A*, astrocytes cultivated under control conditions were fixed and double-stained for GFAP and GLAST or GLT-1. Photomicrographs were taken by confocal imaging. Strong GLAST immunoreactivity was detected mainly at the plasma membrane in virtually all GFAP-positive cells. In contrast, GLT-1 immunoreactivity was hardly detectable in astrocytes. *B*, astrocytes incubated for 3 days with 80 nM of C3bot were fixed and stained for the same antigens. Astrocyte morphology had changed to a stellate appearance. Under these conditions, both GLAST and GLT-1 were detectable in GFAP-positive cells and also localized to very thin processes. *C*, incubation with DHK prevents C3bot-mediated enhanced [^{3}H]glutamate uptake. Prior to the uptake procedure, astrocytes were preincubated for 30 min with two concentrations of DHK. In control cultures, DHK had no effect on glutamate uptake. Conversely, higher glutamate uptake in C3bot-treated cultures was reduced to control levels by DHK.

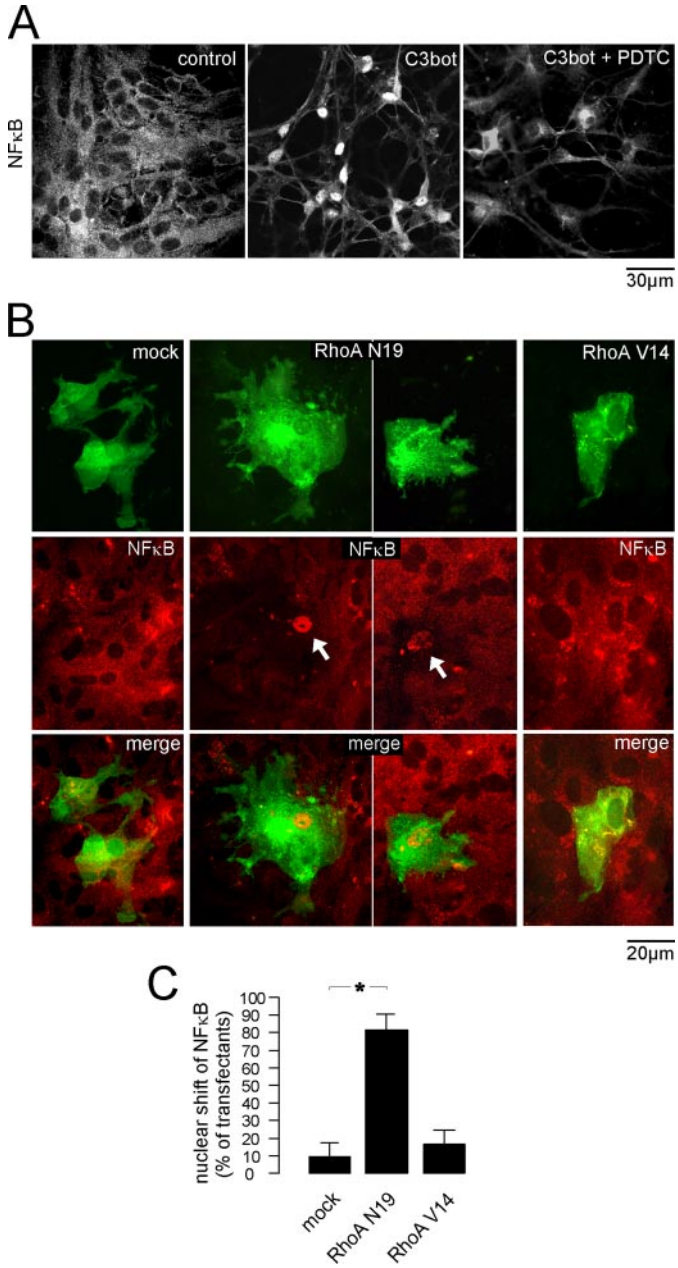

FIGURE 3. **Inhibition of Rho activity induces nuclear translocation of transcription factor NFκB.** *A*, C3bot induces NFκB translocation to the nucleus. Confocal images of astrocytes stained for the p65 subunit of NFκB. In control cultures, NFκB mainly localized to the cytoplasm. After incubation with C3bot (80 nM, 72 h), astrocytes adopted a stellate morphology and exhibited a shift of NFκB to the nuclear region. This effect was prevented by the addition of PDTC (10 μM) during incubation with C3bot. *B*, astrocyte cultures were transfected with RhoA constructs cloned into pEGFP vector and stained for NFκB immunoreactivity. Transfection with dominant negative RhoA N19 (depicted are two transfected cells from two different cultures) resulted in NFκB translocation to the nucleus (*arrows*). Transfection with constitutively active RhoA V14 as well as mock transfection had no effect on cytoplasmatic NFκB localization. *C*, quantitative analysis of the observed phenotype (nuclear shift of NFκB) in transfected astrocytes.

the quencher agent SCAS to remove background staining. Following quenching, cells were fixed as described above, followed by an additional 4′,6-diamidino-2-phenylindole staining procedure. For quantification of fluorescent spots, AM1-43 puncta of 50–250 pixels (0.57–2.86 μm^2) detected within individual view fields of 136 × 108 μm were counted by using Scion Image software. Counts were adjusted to cell numbers as revealed by 4′,6-diamidino-2-phenylindole staining. In a single experiment, between 400 and 500 cells were analyzed per condition.

Experimental Design and Statistics

Experiments were run at least three times. Uptake and secretion assays were determined in triplicates for a single condition. In general, values are expressed as means ± S.D. from one representative experiment if not stated otherwise. Statistical sig-

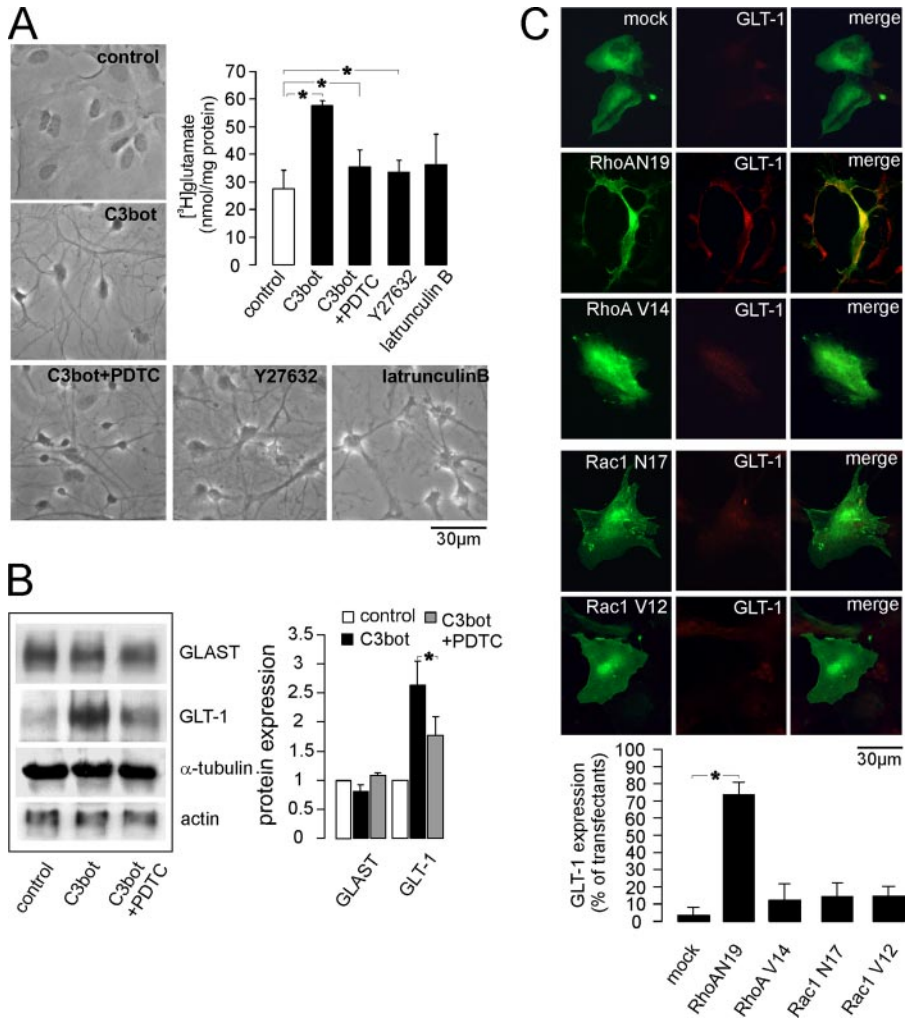

FIGURE 4. **Enhanced glutamate uptake and GLT-1 up-regulation represents a Rho-specific effect mediated by NFκB.** *A*, astrocyte cultures were incubated without (control) or with C3bot (80 nM), C3bot and PDTC (10 μM), the Rho-kinase inhibitor Y27632 (10 μM), or latrunculin B (1 μM) for 72 h. All treatments resulted in strong morphological shape changes toward a ramified morphology. In parallel, uptake experiments using [^{3}H]glutamate (50 μM) were performed. The combined treatment of C3bot and PDTC resulted in a strongly reduced uptake compared with cultures treated with C3bot alone. Treatment with Y27632 enhanced glutamate uptake to a moderate, yet significant, extent. Latrunculin B had no significant effect on the uptake. *B*, Western blot analysis of GLAST and GLT-1 expression from cultures treated as above. α-Tubulin and actin were used as internal standards. Quantification of signals (normalized to α-tubulin) revealed a strong up-regulation of GLT-1 after application of C3bot. This effect was significantly reduced by PDTC. GLAST levels remained largely unaffected. *C*, astrocyte cultures were transfected with RhoA constructs cloned into pEGFP vector and stained for GLT-1 immunoreactivity. Transfection with dominant negative RhoA N19 resulted in GLT-1 up-regulation in a large proportion of transfectants as shown in the diagram. Transfection with either constitutively active RhoA V14, Rac1 V12, or dominant negative Rac1 17N had no significant effect.

nificance was calculated using Student's *t* test, and *p* values below 0.05% were considered significant.

RESULTS

The effect of C3bot on the glutamate uptake was studied by incubation of astrocytes pretreated with 80 nM C3bot for 6, 12, 24, or 72 h with 50 μM [^{3}H]glutamate. The specificity of glutamate uptake was confirmed by inhibition of the plasma membrane glutamate transporter activity by PDC or threo-β-benzyloxyaspartic acid. C3bot enhanced glutamate uptake by a factor of 1.7 after 24 h compared with control conditions (Fig. 1*A*). After 72 h of C3bot treatment, glutamate uptake was increased by more than 2-fold compared with control conditions. Kinetic analysis of glutamate uptake revealed a higher maximal transport velocity V_{max} and an increased substrate affinity indicated by a lower K_m value in C3bot-treated cultures (Fig. 1*B*). Next we looked for the expression of GLAST and GLT-1, the two high affinity transporter subtypes mediating astrocytic glutamate transport at the plasma membrane. By using confocal laser-scanning microscopy, it became evident that GLAST was expressed at high levels at the plasma membrane of virtually all GFAP-positive control cells (Fig. 2*A*). Conversely, GLT-1 expression was hardly detectable. Upon incubation with 80 nM C3bot, astrocytes changed their morphology toward a stellate shape, as described before (20). After C3bot treatment for 72 h, GLAST expression was still observable, but GLT-1 expression was strongly up-regulated (Fig. 2*B*). Both transporters were detectable also at the fine elongated processes extending from the cell body. To verify whether the C3bot-induced increased glutamate uptake was mainly mediated by GLT-1, astrocytes were preincubated with DHK, a selective GLT-1 inhibitor. Preincubation with 250 or 500 μM DHK for 30 min had no effect on the subsequent glutamate uptake, whereas the enhanced C3bot-induced uptake was exactly reduced to control levels (Fig. 2*C*).

Transcription of the *glt-1* gene is under the control of the NFκB transcription factor (28). To check for a possible effect of C3bot on NFκB activity, we studied the cellular distribution of NFκB in astrocytes. In control cultures, NFκB was mainly in the cytoplasm, detected by immunolabeling using an antibody against the p65 subunit and confocal microscopy (Fig. 3*A*). In astrocytes treated with C3bot for 72 h, a clear shift of p65 from the cytoplasm to the nucleus took place. The C3bot-induced shift was prevented by PDTC (10 μM), an inhibitor of NFκB signaling. Noteworthy, PDTC did not affect C3bot-induced shape changes. To further check whether impairment of Rho activity results in NFκB translocation into the nucleus, we transfected astrocyte cultures with plasmids encoding RhoA proteins. No alterations of the cytoplasmatic localization of NFκB were detected when astrocytes were transfected with either wild type RhoA (not shown) or constitutively active RhoA V14 (Fig. 3, *B* and *C*). Conversely, 80% of astrocytes that expressed dominant negative RhoA N19 exhibited the nuclear

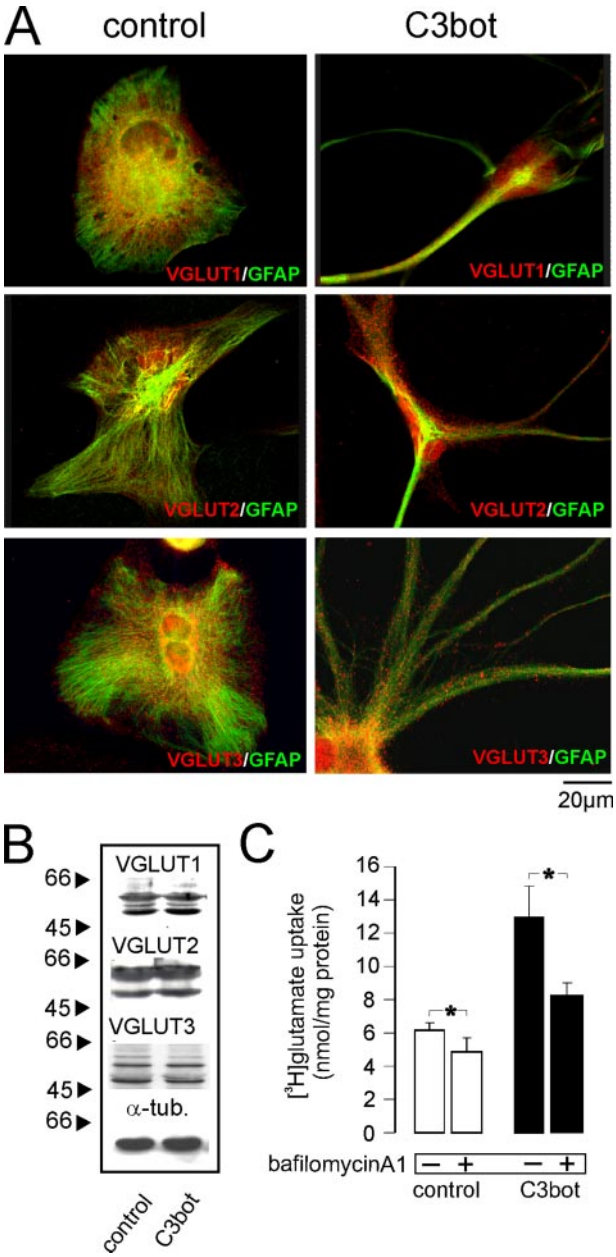

FIGURE 5. **Vesicular glutamate storage contributes to the C3bot-mediated enhanced uptake.** *A*, astrocytes were double-stained for GFAP, and the three vesicular glutamate transporters VGLUT1, -2, and -3. Under either control conditions or after C3bot treatment (80 nM, 72 h), all three vesicular transporters were expressed in a punctate fashion in GFAP-positive cells, including the fine processes of stellate astrocytes. *B*, Western blot analysis of vesicular glutamate transporter expression. Cultures were treated as given above. No changes of overall protein levels of VGLUT1, -2, and -3 were detectable after treatment with C3bot. α-Tubulin was used for loading control. *C*, [3H]glutamate uptake after pretreatment for 1 h with 1 μM bafilomycin A1. Bafilomycin A1 reduced the glutamate uptake in both control and C3bot (80 nM, 72 h) treated astrocyte cultures. The reduction in C3bot-treated cells was more pronounced than under control conditions regarding both absolute and relative values.

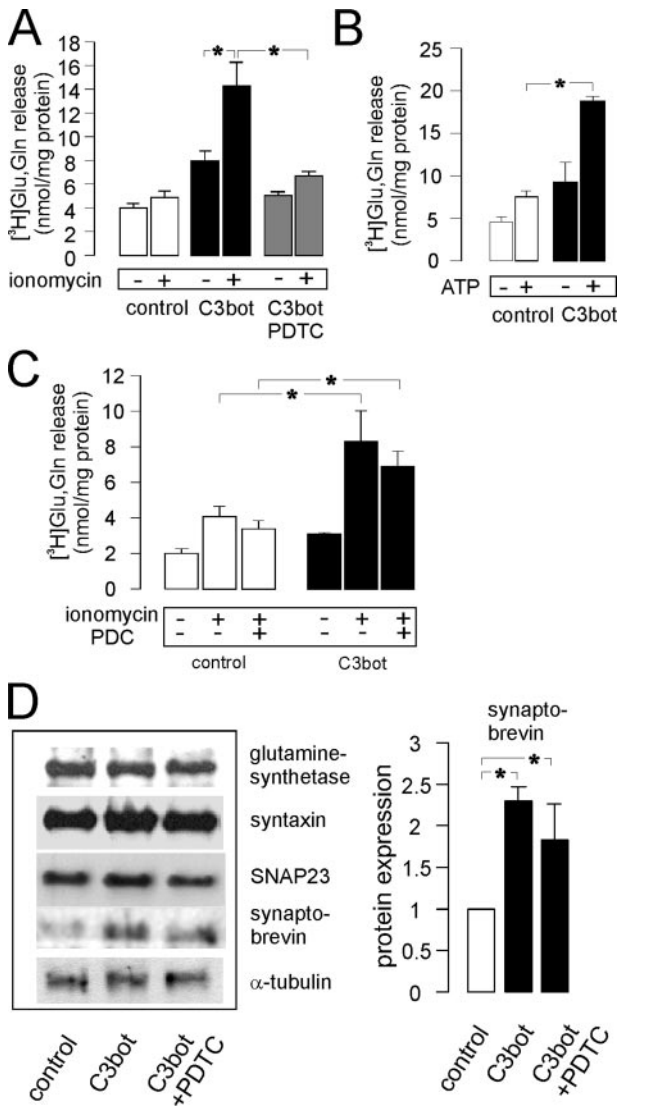

FIGURE 6. **C3bot stimulates glutamate/glutamine release from astrocytes.** *A*, control cultures or astrocytes treated with C3bot (80 nM, 72 h, with or without 10 μM PDTC) were preloaded for 1 h with 50 μM [3H]glutamate. Glutamate secretion was stimulated by the addition of ionomycin (1.3 μM). Supernatants were collected, measured by liquid scintillation counting, and normalized to protein amounts. After incubation with C3bot, ionomycin-induced secretion was significantly increased. This effect was nearly completely prevented by PDTC. *B*, control cultures and cells treated with C3bot were treated with ATP to stimulate release. Compared with control conditions and very similar to ionomycin, ATP (2 mM) stimulated the release of higher amounts of glutamate/glutamine from astrocytes treated with C3bot. *C*, following the uptake procedure, cultures were incubated with PDC (30 min, 1 mM) prior to the stimulation by ionomycin in order to block a putative GLAST/GLT-1-mediated reverse transport. No significant effects on the release were obtainable. *D*, Western blot analysis of SNARE protein expression and glutamine synthetase levels. α-Tubulin was used for loading control. Syntaxin and SNAP23 levels remained largely unaffected after a 72-h incubation period with C3bot or C3bot/PDTC. Synaptobrevin, on the other hand, was detectable at higher levels under either C3bot condition. No alterations in glutamine synthetase signals were detectable.

shift of NFκB. As expected, RhoA N19-expressing cells tended toward development of cellular processes. In sum, the inactivation of Rho by C3bot treatment and the transfection studies clearly indicated a negative regulation of NFκB activity by RhoA in astrocytes.

To address the question of whether enhanced GLT-1 expression and glutamate uptake is based on the Rho-NFκB signaling or is a mere cytoskeletal response, glutamate uptake was performed in C3bot-treated cells in the presence of the NFκB inhibitor PDTC. Cultures that were treated with this combination still exhibited a clear stellate morphology but showed only a moderately increased glutamate uptake that did not reach C3bot levels (Fig. 4*A*). In parallel, we applied the ROCK inhibitor Y27632 (10 μM) to our cultures to study whether this RhoA

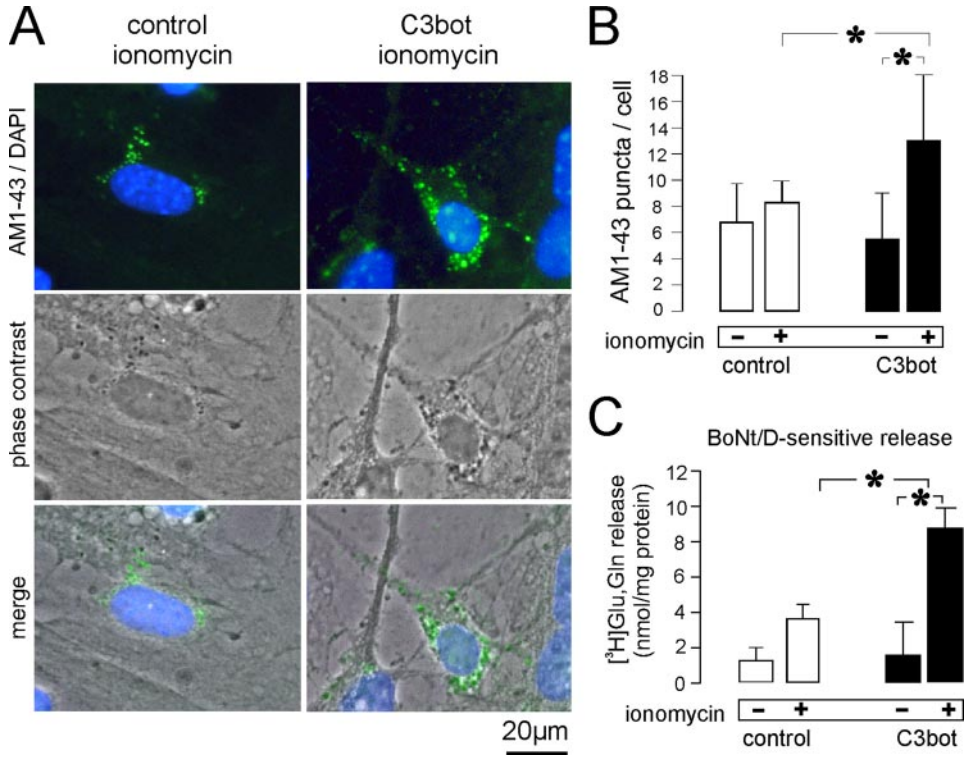

FIGURE 7. **C3bot enhances vesicular exo-endocytotic fusion events with the plasma membrane.** *A*, sample images of ionomycin-stimulated astrocytes cultivated under control conditions or after treatment with 80 nM C3bot for 72 h. Living cells were incubated with a 4 μM concentration of the fixable styryl dye AM1-43. AM1-43 allows for an activity-dependent staining of vesicular trafficking to the plasma membrane. After fixation, astrocytes were additionally stained for 4′,6-diamidino-2-phenylindole to achieve cell counting. Phase-contrast images show the cell morphology. *B*, quantification of AM1-43-stained vesicles (given in puncta per cell). Ionomycin increases the number of AM1-43 stained puncta, especially in C3bot-treated cultures. *C*, control cultures or cultures treated with C3bot were incubated with 1 nM BoNt/D for 24 h prior to release experiments. Values obtained from cells pretreated with BoNt/D were subtracted from the ones without BoNt/D treatment to calculate BoNt/D-sensitive and therefore exocytotic release. Ionomycin-stimulated exocytosis was significantly enhanced in C3bot-treated astrocytes.

downstream effector that mainly regulates actin dynamics is involved. Besides changes toward a stellate morphology, glutamate uptake itself, however, only reached slightly enhanced levels. Additionally, we used the sponge toxin latrunculin B, an F-actin depolymerizing agent that acts independently from Rho pathways (29). Astrocytes incubated with 1 μM latrunculin B developed the expected stellate morphology but failed to show any significantly enhanced glutamate uptake (Fig. 4*A*).

To check whether the effects of PDTC on C3bot-enhanced glutamate uptake levels were due to an inhibition of glutamate transporters, GLAST and GLT-1 expression were compared in control cells, cells treated with C3bot alone or in combination with PDTC (Fig. 4*B*). Under control conditions, GLT-1 was detectable at very low amounts but was found to be strongly up-regulated (2.7-fold) by C3bot. The addition of PDTC prevented the C3bot-triggered up-regulation to a large extent. GLAST levels were only moderately lowered by C3bot. To further support the up-regulation of GLT-1 by a Rho-dependent mechanism, we transfected astrocytes with RhoA constructs (Fig. 4*C*). In line with the results shown for NFκB (Fig. 3, *B* and *C*), only expression of dominant negative RhoA N19 was able to induce GLT-1 up-regulation in the majority (74%) of transfected cells. Again, many astrocytes transfected with RhoA N19 showed a branched morphology. In addition, we performed transfection studies with wild type, constitutively active and dominant negative Rac1 (not shown). No pronounced effects on GLT-1 expression were detected, confirming the specificity of RhoA effects (Fig. 4*C*).

Besides their high affinity plasma membrane glutamate transporters, astrocytes harbor vesicular compartments capable of glutamate storage mediated by the vesicular glutamate transporters VGLUT1 to -3. To check the C3bot effect on the vesicular transport systems we examined VGLUT expression. VGLUT1, -2, and -3 were detectable in a punctate distribution in a large proportion of GFAP-positive astrocytes, as shown by immunocytochemistry (Fig. 5*A*). VGLUT-immunoreactive puncta were found all over the cells, including the processes in cells treated with C3bot. In parallel, VGLUT expression was analyzed by Western blotting. No alterations in total protein levels of VGLUT1, -2, and -3 by C3bot were detectable (Fig. 5*B*). These findings, however, do not exclude possible changes in VGLUT activity by regulatory mechanisms apart from an altered protein synthesis. To investigate the contribution of vesicular uptake to the overall glutamate uptake, astrocytes were incubated with bafilomycin A1 prior to the uptake procedure. Bafilomycin A1 inhibits the vacuolar ATPase activity and therefore prevents acidification of storage vesicles. In control cultures, a treatment with 1 μM bafilomycin A1 for 1 h inhibited glutamate uptake by 25% (Fig. 5*C*). Remarkably, the C3bot-induced enhanced glutamate uptake was reduced by 40%, indicating a higher vesicular transport.

Glutamate taken up by astrocytes can be converted to glutamine by the astroglial glutamine synthetase or may also be secreted again into the extracellular space. To test whether inhibition of Rho pathways by C3bot affects glutamate release and the putative co-release of glutamine, we applied the following stimulation paradigm. The Ca^{2+} ionophore ionomycin raises intracellular Ca^{2+} levels, thereby stimulating release mechanisms. In a first attempt, release of radioactivity from control cells as well as from C3bot-treated cells (with or without the addition of PDTC) was analyzed irrespective of the nature of the released substances. In control cultures incubated with [^{3}H]glutamate for 1 h, ionomycin (1.3 μM) raised basal release from 4 to 4.9 nmol/mg protein (Fig. 6*A*). After C3bot treatment (72 h, 80 nM), release following stimulation was enhanced by a factor of 1.8 from 7.9 nmol/mg protein (control) to 14.3 nmol/mg protein (ionomycin). The addition of PDTC during incubation with C3bot reduced the enhanced ionomy-

cin-stimulated release almost completely to control levels. Furthermore, we investigated the effect of C3bot on ATP-stimulated release, a physiological compound that is well known to stimulate glutamate release from astrocytes. Comparable with the data for ionomycin, incubation with C3bot also enhanced both basal and especially ATP-stimulated release (Fig. 6*B*). To address the question of whether a reverse transport by plasma membrane transporters might contribute to the enhanced release, we incubated our cultures with PDC (1 mM) for 30 min subsequent to the uptake and prior to the stimulation procedure. No significant reduction of the ionomycin-stimulated release was observed under either condition (Fig. 6*C*).

A large body of evidence has accumulated demonstrating that astrocytes contain the constituents of the SNARE complex, and glutamate is also being released from astrocytes by secretory vesicles undergoing exocytosis (7, 30). To detect possible changes in the exocytotic core machinery, we checked for the level of syntaxin, SNAP23, synaptobrevin, and glutamine synthetase, the enzyme responsible for the glutamate-glutamine conversion. Although syntaxin and SNAP23 levels showed only minor alterations by C3bot after 72 h (with or without PDTC), synaptobrevin was significantly up-regulated by C3bot (Fig. 6*D*). No changes in glutamine synthetase levels were detectable.

Both the data from the bafilomycin A1 uptake experiments as well as the release experiments point to an enhanced contribution of vesicular glutamate storage and Ca^{2+}-dependent secretion following C3bot treatment. To study the occurrence of vesicular exo-endocytotic events in astrocytes, we incubated the cultures with the fixable fluorescent styryl dye AM1-43 that becomes trapped in vesicular membranes in an activity-dependent fashion. In our experimental design, we incubated astrocytes with 4 μM of AM1-43 with or without ionomycin. The increase in fluorescent puncta reflects increased vesicular fusion events with the plasma membrane. In the absence of ionomycin, the number of fluorescent vesicles (or vesicle clusters) of control cells did not significantly differ from the C3bot-treated ones (Fig. 7, *A* and *B*). The addition of ionomycin extensively increased the number of AM1-43-stained puncta in C3bot-treated cells, whereas those from control cultures only moderately increased. To differentiate between vesicular and nonvesicular release, we blocked exocytotic membrane fusion events by preincubating astrocytes for 24 h prior to glutamate/glutamine release exper-

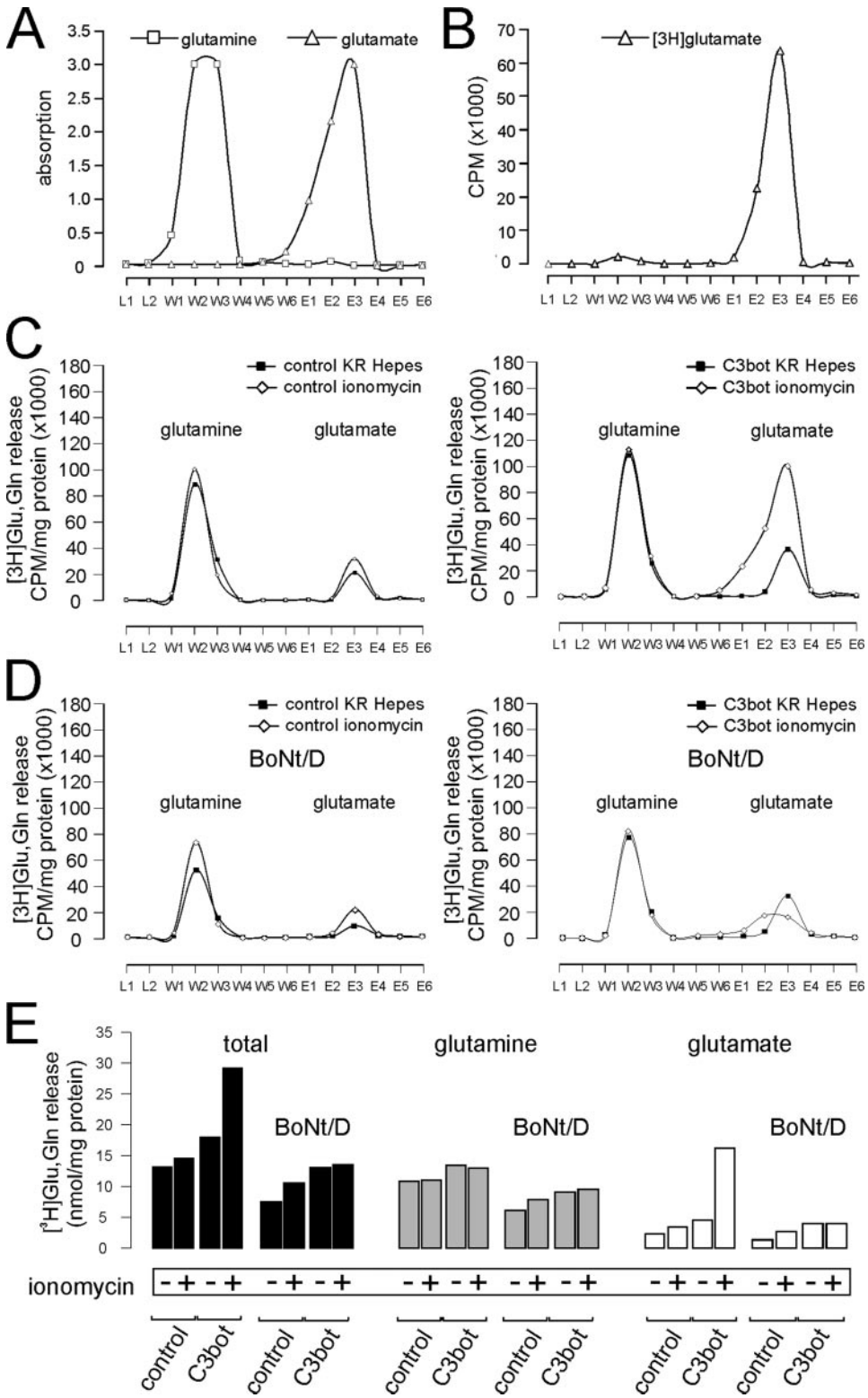

iments with BoNt/D (1 nM), thereby cleaving synaptobrevin/cellubrevin. By subtracting the remaining BoNt/D-insensitive from total values, the BoNt/D-sensitive, namely exocytotic, values were obtained (Fig. 7*C*). Treatment with C3bot had no effect on basal vesicular release but significantly enhanced ionomycin-stimulated exocytotic release, further supporting the AM1-43 experiments.

To distinguish between Rho-dependent effects on both glutamate and glutamine release, we analyzed culture supernatants by ion exchange chromatography. We took advantage of the different charges of glutamate and glutamine at defined pH values. In control experiments, we first figured out the adequate condition allowing the complete separation of glutamate from glutamine. Using a Sepharose matrix as a strong anion exchanger, we loaded either unlabeled glutamine or glutamate (20 mM each) onto separate columns at a pH of 6.0, followed by washing steps at the same pH value and subsequent elution at a pH of 3.7. Amine groups of glutamine and glutamate were determined photometrically from the collected fractions. Due to its positive charge at pH 6.0, glutamine was completely washed out during the washing steps (Fig. 8*A*). The negatively charged glutamate bound at this pH value was quantitatively eluted when lowering the pH to 3.7. These results were further confirmed for glutamate by using radiolabeled 50 μM glutamate, the concentration used in our experiments (Fig. 8*B*). We now loaded supernatant samples from release experiments (performed with ionomycin as described before) onto the columns and determined the radioactivity of collected fractions. Under control conditions, both buffer-treated and ionomycin-stimulated astrocytes secreted mainly glutamine (around 80%) and only small amounts of glutamate (Fig. 8*C*, *left*; see also Fig. 8*E*). Ionomycin slightly stimulated total release, as observed before, leaving the ratio between glutamine and glutamate unaffected. As expected, astrocytes incubated with C3bot (Fig. 8*C*, *right*; see also Fig. 8*E*) exhibited a higher overall release, compared with control cells, leaving the relative proportions of glutamine and glutamate mainly unaffected. Stimulation with ionomycin increased mainly glutamate release, which now reached 56% of total release. Glutamate therefore exclusively accounted for the enhanced release following stimulation in C3bot-treated cells.

To differentiate between vesicular and nonvesicular release, we again used BoNt/D (24 h, 1 nM) to inhibit exocytotic release. In control cells, both buffer-treated and ionomycin-stimulated cells secreted less glutamate and glutamine (Fig. 8*D*; see also Fig. 8*E*), the latter being at most reduced by 4 nmol/mg protein. The high glutamate levels detected in ionomycin-stimulated cells without BoNt/D preincubation were strongly reduced by 75% and comparable with buffer-treated values after blocking exocytosis. Also, glutamine levels were reduced by 25–30%.

DISCUSSION

Inhibition of Rho signaling resulted in a robust up-regulation of GLT-1 expression and increased glutamate uptake, whereas GLAST expression remained largely unaffected. Transfection experiments with dominant negative RhoA N19 as well as uptake experiments with different stellation-inducing compounds, including latrunculin B, strongly support a Rho-specific effect on GLT-1 up-regulation. Expression and activity of both transporter subtypes have been shown to be highly variable. Factors, among them glutamate itself, that change protein levels and performance of glutamate uptake can be neuron-derived (31, 32). Also, endogenous Akt (protein kinase B) induces GLT-1 expression through increased transcription but leaves GLAST expression unaffected (33). Another regulatory mechanism that primarily affects GLT-1, representing the major transporter form in the adult rodent brain (34), is the region-specific up-regulation of astrocyte glutamate transport by glucocorticoids (35). Given the fact that increased GLT-1 expression often accompanies a general change to a more differentiated phenotype, it seems that Rho-dependent signaling cascades are indeed the key players in orchestrating both morphological rearrangements and functional alterations. NFκB was identified as one of the signaling factors downstream of Rho. It has been recently demonstrated that expression of the *eaat2*/*glt-1* gene is under differential control of NFκB (36). In this study, the authors have shown that NFκB can act both as a positive and as a negative regulator of gene expression, depending on the nature of the triggering extracellular signal. Also, a negative regulation of NFκB signaling was demonstrated both for RhoA (37) and RhoB (38) by inhibiting phosphorylation (and degradation) of IκB. In accordance with these data, Rho inactivation by C3bot resulted in the shift of NFκB p65 subunit to the nucleus and the subsequent increased GLT-1 expression (this paper). Nevertheless, it has been shown that Rho proteins might also have activating effects on NFκB depending probably on the cell type (39). The fact that inhibition of ROCK activity by Y27632 had only moderate effects on glutamate uptake indicates that this pathway is not crucially involved in NFκB activation.

The results from the bafilomycin A1 experiments indicate that vesicular transport mechanisms significantly contribute to

FIGURE 8. **C3bot mainly enhances Ca^{2+}-dependent, botulinum neurotoxin D-sensitive glutamate release from astrocytes.** *A*, separation of glutamine and glutamate by ion exchange chromatography. Glutamine and glutamate (20 mM each) were loaded on separate anion-exchanging Sepharose Q columns equilibrated with sample buffer at a pH value of 6.0. After collection of loading fractions (*L*) followed by six washing steps (*W*) with sample buffer, columns were eluted with 6 volumes of elution buffer (*E*) at a pH of 3.7. Amine groups were detected photometrically. As shown, a complete separation of glutamine from glutamate was achieved. *B*, determination of [^{3}H]glutamate by liquid scintillation counting. [^{3}H]glutamate at 50 μM was loaded onto a column, and radioactivity was determined from collected fractions. The graph indicates the complete elution within fractions E1–E4. *C*, determination of [^{3}H]glutamine and [^{3}H]glutamate from astrocyte supernatants. Astrocytes were incubated with or without the addition of 80 nM C3bot for 72 h and incubated with 50 μM [^{3}H]glutamate for 1 h. Release was stimulated using either buffer alone or ionomycin (1.3 μM). Supernatants were taken and subjected to ion exchange chromatography. Control cells (*left*) released predominantly glutamine and smaller amounts of glutamate. Incubation with C3bot (*right*) led to an increased release of both substances. Most noteworthy, ionomycin-stimulated glutamate release was strongly up-regulated. *D*, preincubation of astrocytes with BoNt/D. Prior to stimulation, astrocytes were peincubated with BoNt/D (1 nM, 24 h) to prevent exocytotic release events. In control cells, BoNt/D reduced both the release of glutamine and glutamate. In C3bot-treated astrocytes, ionomycin-stimulated release of glutamate was inhibited to the highest degree. *E*, quantification of [^{3}H]glutamine and [^{3}H]glutamate release from collected fractions. *A–E*, data represent values from one representative experiment. In a second independent experiment, data were confirmed.

the overall uptake, especially in astrocytes incubated with C3bot. Since protein levels of all three VGLUTs detected in our culture were not increased after C3bot application, other regulatory mechanisms might account for an enhanced C3bot-mediated vesicular uptake. VGLUT activity is regulated by the α-subunit of the heterotrimeric G protein Go2, which changes its chloride dependence (40). Also, posttranslational modifications of transporter proteins might occur.

C3bot-mediated Rho inhibition also promoted Ca^{2+}-dependent glutamate release. As demonstrated by BoNt/D, this release mainly occurs by exocytosis. Glutamate release by astrocytes has drawn strong attention, since astrocytes are able to modulate synaptic transmission by glutamate release (30). It became evident that astrocytes express functional core components of the exocytotic machinery (7, 41, 42). Functionally, it was shown that glutamate released by exocytosis from astrocytes enhances synaptic strength of excitatory synapses of the dentate gyrus (12). The precise mechanism by which C3bot-mediated impairment of Rho signaling leads to enhanced exocytotic glutamate release is not known so far. Nevertheless, up-regulation of at least the SNARE protein synaptobrevin is likely to contribute to the enhanced exocytosis. NFκB appears not to be essentially involved in this up-regulation. Changes in the availability of Ca^{2+} as a trigger stimulus as well as cytoskeletal rearrangements are possible, since Rho is the master regulator of the actin cytoskeleton. A contribution of actin depolymerization to the facilitation of docking and fusion of secretory vesicles with the plasma membrane has been demonstrated for chromaffin cells (43). In neurons, stabilization of actin filaments (which is prevented by C3bot) reduces the amount of neurotransmitter released from the reserve pool (44). Another finding that supports a negative regulation of exocytosis by Rho proteins comes from the fact that expression of nadrin, a neuronal GTPase-activating protein, enhances exocytosis in PC12 cells (45).

Secreted glutamine was also moderately elevated in C3bot-treated cells. This corresponds well with a recent observation that the efflux of glutamine from astrocytes by the main transporter SNAT3 (system N) is positively regulated by increased intracellular glutamate concentrations. The mechanism for this is thought to be a higher affinity of SNAT3 for its substrate (46). Therefore, the observed effect might represent an indirect consequence of Rho inhibition by C3bot, leading to higher glutamate concentrations and subsequently also to an enhanced glutamine release. Another observation we made was the down-regulation of glutamine release after blocking exocytosis by BoNt/D. Hitherto, there is no evidence for vesicular storage (and release) of glutamine in any cell type. One reason for this discrepancy might be an impaired trafficking of efflux systems (*e.g.* SNAT3) to the plasma membrane after blocking membrane fusion events with BoNt/D.

Finally, the application of C3bot to foster neuronal regeneration, as it is currently considered, concomitantly results in up-regulation of glutamate uptake. This fact might be beneficial under those central nervous system pathologies that are associated with impaired glutamate uptake by astrocytes like amyotrophic lateral sclerosis or Alzheimer disease (47, 48). Because C3bot also promotes exocytotic glutamate release, this effect might therefore antagonize an increased uptake under circumstances when astrocytes are stimulated to secrete glutamate.

In summary, the present study demonstrates that inhibition of Rho-dependent signaling pathways by *C. botulinum* C3 protein leads to an increased glutamate uptake mediated by NFκB-dependent up-regulation of GLT-1 and a vesicular transport mechanism. At the same time, the potency for the secretion of glutamine and, more pronounced, glutamate in a mainly exocytotic fashion is enhanced.

Acknowledgments—We thank Birgit Metze and Suzan Öztürk for expert technical assistance.

REFERENCES

1. Lehre, K. P., and Danbolt, N. C. (1998) *J. Neurosci.* **18,** 8751–8757
2. Ventura, R., and Harris, K. M. (1999) *J. Neurosci.* **19,** 6897–6906
3. Choi, D. W. (1988) *Neuron* **8,** 623–634
4. Rothstein, J. D., Dykes-Hoberg, M., Pardo, C. A., Bristol, L. A., Jin, L., Kuncl, R. W., Kanai, Y., Hediger, M. A., Wang, Y., Schielke, J. P., and Welty, D. F. (1996) *Neuron* **3,** 675–686
5. Danbolt, N. C. (2001) *Prog. Neurobiol.* **1,** 1–105
6. Montana, V., Ni, Y., Sunjara, V., Hua, X., and Parpura, V. (2004) *J. Neurosci.* **11,** 2633–2642
7. Bezzi, P., Gundersen, V., Galbete, J. L., Seifert, G., Steinhauser, C., Pilati, E., and Volterra, A. (2004). *Nat. Neurosci.* **6,** 613–620
8. Chen, X., Wang, L., Zhou, Y., Zheng, L. H., and Zhou, Z. (2005) *J. Neurosci.* **40,** 9236–9243
9. Shiga, H., Murakami, J., Nagao, T., Tanaka, M., Kawahara, K., Matsuoka, I., and Ito, E. (2006) *J. Neurosci. Res.* **2,** 338–347
10. Takano, T., Kang, J., Jaiswal, J. K., Simon, S. M., Lin, J. H., Yu, Y., Li, Y., Yang, J., Diesel, G., Zielke, H. R., and Nedergaard, M. (2005) *Proc. Natl. Acad. Sci. U. S. A.* **45,** 16466–16471
11. Iino, M., Goto, K., Kakegawa, W., Okado, H., Sudo, M., Ishiuchi, S., Miwa, A., Takayasu, Y., Saito, I., Tsuzuki, K., and Ozawa, S. (2001) *Science* **5518,** 926–929
12. Jourdain, P., Bergersen, L. H., Bhaukaurally, K., Bezzi, P., Santello, M., Domercq, M., Matute, C., Tonello, F., Gundersen, V., and Volterra, A. (2007) *Nat. Neurosci.* **3,** 331–339
13. Nägler, K., Mauch, D. H., and Pfrieger, F. W. (2001) *J. Physiol.* **533.3,** 665–679
14. Ullian, E. M., Barkis, W. B., Chen, S., Diamond, J. S., and Barres, B. A. (2004) *Mol. Cell Neurosci.* **4,** 544–557
15. Rothman, D. L., Behar, K. L., Hyder, F., and Shulman, R. G. (2003) *Annu. Rev. Physiol.* **65,** 401–427
16. Gegelashvili, G., and Schousboe, A. (1997) *Mol. Pharmacol.* **1,** 6–15
17. Sattler, R., and Rothstein, J. D. (2006) *Handb. Exp. Pharmacol.* **175,** 277–303
18. Ramakers, G. J., and Moolenaar, W. H. (1998) *Exp. Cell Res.* **2,** 252–262
19. Abe, K., and Misawa, M. (2003) *Brain Res. Dev. Brain Res.* **1,** 99–104
20. Höltje, M., Hoffmann, A., Hofmann, F., Mucke, C., Grosse, G., Van Rooijen, N., Kettenmann, H., Just, I., and Ahnert-Hilger, G. (2005) *J. Neurochem.* **5,** 1237–1248
21. Boquet, P., Munro, P., Fiorentini, C., and Just, I. (1998) *Curr. Opin. Microbiol.* **1,** 66–74
22. Aktories, K., and Just, I. (2005) *Curr. Top. Microbiol. Immunol.* **291,** 113–145
23. Vogelsgesang, M., Pautsch, A., and Aktories, K. (2007) Naunyn Schmiedeberg's *Arch. Pharmacol.* **5–6,** 347–360
24. Fischer, D., Petkova, V., Thanos, S., and Benowitz, L. I. (2004) *J. Neurosci.* **40,** 8726–8740
25. Bertrand, J., Di Polo, A., and McKerracher, L. (2007) *Neurobiol. Dis.* **1,** 65–72
26. Fields, R. (1971) *Biochem. J.* **124,** 581–590
27. Renger, J. J., Egles, C., and Liu, G. (2001) *Neuron* **2,** 469–484
28. Rodriguez-Kern, A., Gegelashvili, M., Schousboe, A., Zhang, J., Sung, L.,

and Gegelashvili, G. (2003) *Neurochem. Int.* **4,** 363–370
29. Spector, I., Shochet, N. R., Blasberger, D., and Kashman, Y. (1989) *Cell Motil. Cytoskeleton.* **3,** 127–144
30. Araque, A., Parpura, V., Sanzgiri, R. P., and Haydon, P. G. (1998) *Eur. J. Neurosci.* **6,** 2129–2142
31. Swanson, R. A., Liu, J., Miller, J. W., Rothstein, J. D., Farrell, K., Stein, B. A., and Longuemare, M. C. (1997) *J. Neurosci.* **3,** 932–940
32. Poitry-Yamate, C. L., Vutskits, L., and Rauen, T. (2002) *J. Neurochem.* **4,** 987–997
33. Li, L. B., Toan, S. V., Zelenaia, O., Watson, D. J., Wolfe, J. H., Rothstein, J. D., and Robinson, M. B. (2006) *J. Neurochem.* **3,** 759–771
34. Tanaka, K., Watase, K., Manabe, T., Yamada, K., Watanabe, M., Takahashi, K., Iwama, H., Nishikawa, T., Ichihara, N., Kikuchi, T., Okuyama, S., Kawashima, N., Hori, S., Takimoto, M., and Wada, K. (1997) *Science* **5319,** 1699–1702
35. Zschocke, J., Bayatti, N., Clement, A. M., Witan, H., Figiel, M., Engele, J., and Behl, C. (2005) *J. Biol. Chem.* **41,** 34924–34932
36. Sitcheran, R., Gupta, P., Fisher, P. B., and Baldwin, A. S. (2005) *EMBO J.* **3,** 510–520
37. Rattan, R., Giri, S., Singh, A. K., and Singh, I. (2003) *Free Radic. Biol. Med.* **9,** 1037–1050
38. Fritz, G., and Kaina, B. (2001) *J. Biol. Chem.* **5,** 3115–3122
39. Perona, R., Montaner, S., Saniger, L., Sánchez-Pérez, I., Bravo, R., and Lacal, J. C. (1997) *Genes Dev.* **11,** 463–475
40. Winter, S., Brunk, I., Walther, D. J., Höltje, M., Jiang, M., Peter, J. U., Takamori, S., Jahn, R., Birnbaumer, L., and Ahnert-Hilger, G. (2005) *J. Neurosci.* **18,** 4672–4680
41. Parpura, V., Fang, Y., Basarsky, T., Jahn, R., and Haydon, P. G. (1995) *FEBS Lett.* **3,** 489–492
42. Bezzi, P., Carmignoto, G., Pasti, L., Vesce, S., Rossi, D., Rizzino, B. L., Pozzan, T., and Volterra, A. (1998) *Nature* **6664,** 281–285
43. Vitale, M. L., Seward, E. P., and Trifaro, J. M. (1995) *Neuron.* **2,** 353–363
44. Bernstein, B. W., DeWit, M., and Bamburg, J. R. (1998) *Brain Res. Mol. Brain Res.* **1,** 236–251
45. Harada, A., Furuta, B., Takeuchi, K., Itakura, M., Takahashi, M., and Umeda, M. (2000) *J. Biol. Chem.* **275,** 36885–36891
46. Bröer, A., Deitmer, J. W., and Bröer, S. (2004) *Glia* **4,** 298–310
47. Sasaki, S., Komori, T., and Iwata, M. (2000) *Acta Neuropathol.* (*Berl.*) **100,** 138–144
48. Gegelashvili, G., Robinson, M. B., Trotti, D., and Rauen, T. (2001) *Prog. Brain Res.* **132,** 267–286